Simplitigs as an efficient and scalable representation of de Bruijn graphs

Karel Brinda, Michael Baym, Gregory Kucherov

Simplitigs as an efficient and scalable representation of de Bruijn graphs

Karel Břinda[1,2,*], Michael Baym[1,$], and Gregory Kucherov[3,4,$]

1   Department of Biomedical Informatics, Harvard Medical School, Boston, USA

2   Center for Communicable Disease Dynamics, Department of Epidemiology, Harvard T.H. Chan School of Public Health, Boston, USA

3   CNRS/LIGM Univ Gustave Eiffel, Marne-la-Vallée, France

4   Skolkovo Institute of Science and Technology, Moscow, Russia

*   The corresponding author: karel.brinda@hms.harvard.edu

$ These authors contributed equally to this work

Abstract

De Bruijn graphs play an essential role in computational biology. However, despite their widespread use, they lack a universal scalable representation suitable for different types of genomic data sets. Here, we introduce simplitigs as a compact, efficient and scalable representation and present a fast algorithm for their computation. On examples of several model organisms and two bacterial pan-genomes, we show that, compared to the best existing representation, simplitigs provide a substantial improvement in the cumulative sequence length and their number, especially for graphs with many branching nodes. We demonstrate that this improvement is amplified with more data available. Combined with the commonly used Burrows-Wheeler Transform index of genomic sequences, simplitigs substantially reduce both memory and index loading and query times, as illustrated with large-scale examples of GenBank bacterial pan-genomes.

Keywords

Sequence analysis, de Bruijn graphs, k-mers, representation, scaling

Background

24 Advances in DNA sequencing started the golden age of biology when previously unobservable phenomena can be

25 studied on an unprecedented scale. However, sequencing capacity has been growing faster than computer

26 performance and memory, and also faster than available human resources. Today large amounts of sequence data

27 are available. Consequently, traditional sequence-based representations and sequence alignment-based techniques

28 [1–3] have become less suitable for real-life scenarios due to the space- and time-complexities they impose and

29 their inefficiency in handling polymorphisms.

30

31 De Bruijn graphs provide an elegant solution for genomic data representation. They build on top of the concept of k

32 -mers, which are substrings of a fixed length k of the genomic strings to be represented, such as sequencing reads,

33 genomes, or transcriptomes. For a given k-mer set, the corresponding de Bruijn graph is a directed graph with the

34 k-mers being vertices and $k-1$ long overlaps between pairs of these k-mers indicating edges (Methods). There is

35 an obvious correspondence between k-mer sets and de Bruijn graphs, and we can use both terms interchangeably.

36 If k is chosen appropriately, de Bruijn graphs capture substantial information about the sequenced molecules as

37 these correspond to some walks in the graph.

38

39 The use of de Bruijn graphs is ubiquitous in sequence analysis. Genome assembly uses the property that sequenced

40 molecules form paths [4–6], which is exploited in numerous modern assemblers [7–12]. On the other hand,

41 alignment-free sequence comparison follows the idea that similar sequences share common k-mers, and

42 comparing de Bruijn graphs provides thus a good measure of sequence similarity [13]. This involves applications of

43 de Bruijn graphs to variant calling and genotyping [14–18], transcript abundance estimation [19], and metagenomic

44 classification [20–23]. In the latter application, k-mer-based classifiers perform best among all classifiers in

45 inferring abundance profiles [24], which suggests that de Bruijn graphs truthfully approximate the graph structures

46 of bacterial pan-genomes, even if constructed from noisy assemblies from incomplete databases. Even if more

47 advanced pan-genome graph representations are available, such as variation graphs [25], de Bruijn graphs with

48 large k-mer lengths are still useful for indexing [26,27].

49

50 As de Bruijn graphs are one of the primary data structures in much of sequence analysis, the efficiency of many

51 algorithms is directly tied to the efficiency of computation and representation of the graph. De Bruijn graphs can be

52 readily computed through a scan of the datasets including the raw reads, genomes or multiple sequence files. In

53 practice, such a scan often consists in k-mer counting as this allows efficient denoising of the graph, e.g., by

54 removing low-frequency k-mers corresponding to sequencing errors in the reads. Algorithms for k-mer counting

55 have been extensively studied and many well-engineered software solutions are available [28–36].

56

57 On the other hand, de Bruijn graph representations have received much less attention. The most commonly used

58 representation are unitigs, which are strings resulting from compaction of k-mers along maximal paths with

59 non-branching nodes [37,38]. Unitigs have many advantages: the representation is "textual", in the form of a set of

60 sequences that contain each k-mer exactly once while preserving graph topology. However, unitigs impose large

61 resource overhead for many types of de Bruijn graphs and do not scale well when a lot of variation is included.

62 Specifically, with a high proportion of branching nodes, unitigs become fragmented, in an extreme case up to the

63 level of individual k-mers. Subsequently, unitig computation and storage may require inappropriately large

64 resources and become prohibitive in variation-heavy applications, e.g., in bacterial pan-genomics.

65

66 In this paper, we propose simplitigs as a compact, efficient and scalable representation of de Bruijn graphs.

67 Simplitigs generalize the unitig representation by relaxing the restriction of stopping at branching nodes. We

68 present an algorithm for rapid simplitig computation from a k-mer set and implement it in a tool called ProphAsm.

69 ProphAsm proceeds by loading a k-mer set into memory and a greedy enumeration of maximal vertex-disjoint

70 paths in the associated de Bruijn graph. We use ProphAsm to evaluate the improvement of simplitigs over unitigs,

71 in terms of two main characteristics: the cumulative sequence length (CL) and the number of sequences (NS). We

72 demonstrate that greedily computed simplitigs are close to theoretical bounds in practical applications and provide,

73 compared to unitigs, a substantial improvement in memory requirements and speed in applications such as k-mer

74 matching.

Results

The concept of simplitigs

We developed the concept of simplitigs to efficiently represent de Bruijn graphs of sequence data (**Fig. 1**).
Simplitigs are a generalization of unitigs and correspond to spellings of vertex-disjoint paths covering a given de
Bruijn graph (**Fig. 1a**, Methods). Consequently, maximal simplitigs are such simplitigs where no two simplitigs can
be merged by a $(k-1)$ overlap (Methods). Note that unitigs and k-mers are also simplitigs, but not maximal in
general (**Fig. 1b**). The main conceptual difference between maximal simplitigs and maximal unitigs is that
simplitigs are not limited by branching nodes, which allows for further compaction, with a benefit increasing
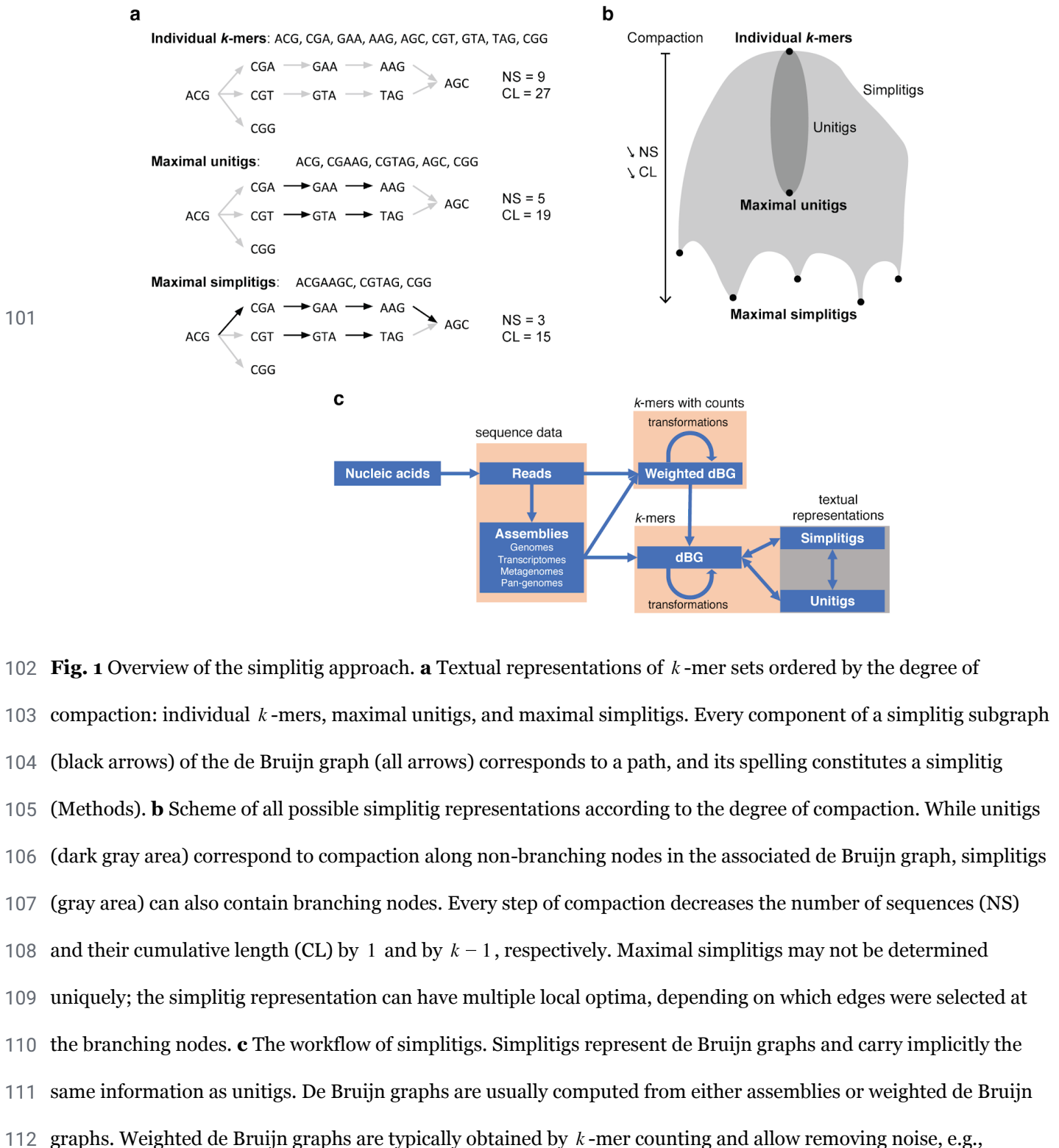proportionally to the amount of branching nodes in the graph.

To compare simplitig and unitig representations, we created a benchmarking procedure based on the two
characteristics: the number of sequences (NS) and their cumulative length (CL) (Methods, example in **Fig. 2**).
While NS determines the number of records to be kept in memory, CL largely determines the total memory needed.
NS and CL are readily bounded from below by one and by the number of k-mers, respectively, and they are also
tightly connected ((eq 1) in Methods). As every step of compaction decreases both NS and CL (**Fig. 1b**, Methods),
we can optimize them jointly. However, finding an optimal simplitig representation translates to the vertex disjoint
path coverage problem. While NP-hard for general graphs (by reduction from the well-known NP-hard problem of
computing a Hamiltonian path), the problem may be tractable for observed de Bruijn graphs (Methods).

Since practical applications do not require optimal simplitigs, we prioritized speed and designed a greedy algorithm
for their rapid computation (**Alg. 1**, Methods). In an iterative fashion, the algorithm selects an arbitrary k-mer as a
seed of a new simplitig and keeps extending it forwards and then backwards as long as possible, while removing the
already used k-mers from the set. This process is repeated until all k-mers are covered. Loading k-mers into
memory and simplitig computation are linear in the length of the input and the number of k-mers, respectively,

4

99 and the memory footprint is linear in the number of k-mers. We implemented **Alg. 1** in a program called

100 ProphAsm, available at https://github.com/prophyle/prophasm.

101

102 **Fig. 1** Overview of the simplitig approach. **a** Textual representations of k-mer sets ordered by the degree of

103 compaction: individual k-mers, maximal unitigs, and maximal simplitigs. Every component of a simplitig subgraph

104 (black arrows) of the de Bruijn graph (all arrows) corresponds to a path, and its spelling constitutes a simplitig

105 (Methods). **b** Scheme of all possible simplitig representations according to the degree of compaction. While unitigs

106 (dark gray area) correspond to compaction along non-branching nodes in the associated de Bruijn graph, simplitigs

107 (gray area) can also contain branching nodes. Every step of compaction decreases the number of sequences (NS)

108 and their cumulative length (CL) by 1 and by $k-1$, respectively. Maximal simplitigs may not be determined

109 uniquely; the simplitig representation can have multiple local optima, depending on which edges were selected at

110 the branching nodes. **c** The workflow of simplitigs. Simplitigs represent de Bruijn graphs and carry implicitly the

111 same information as unitigs. De Bruijn graphs are usually computed from either assemblies or weighted de Bruijn

112 graphs. Weighted de Bruijn graphs are typically obtained by k-mer counting and allow removing noise, e.g.,

113 low-frequency k-mers, which frequently originate in sequencing errors.

114

115 **Alg. 1** Greedy computation of maximal simplitigs for a k-mer set or a de Bruijn graph. In an iterative fashion, the

116 algorithm draws a k-mer from the set of canonical k-mers K, uses it as a seed of a new simplitig, and then keeps

117 extending the simplitig forwards as long as possible, and then backwards, while removing the already used

118 canonical k-mers from K.

```
119  Function extend_simplitig_forwards (K, simplitig):
120          extending = True
121          while extending:
122                  extending = False
123                  q = suffix (simplitig, k-1),
124                  for x in ['A', 'C', 'G', 'T']:
125                          canon_kmer = canonical (q + x)
126                          if canon_kmer in K:
127                                  extending = True
128                                  simplitig = simplitig + x
129                                  K.remove (canon_kmer)
130                                  break
131          return K, simplitig
132
133  Function compute_maximal_simplitig_from_kmer (K, seeding_kmer):
134          simplitig = initial_kmer
135          K, simplitig = extend_simplitig_forwards (K, simplitig)
136          simplitig = reverse_completent (simplitig)
137          K, simplitig = extend_simplitig_forwards (K, simplitig)
138          return K, simplitig
139
140  Function compute_simplitigs (input_kmers):
141          K = {}
142          for kmer in input_kmers:
143                  K.add (canonical (kmer))
144          maximal_simplitigs = {}
145          while |K| > 0:
146                  seeding_kmer = K.pop ()
147                  K, simplitig = compute_maximal_simplitig_from_kmer (K, seeding_kmer)
148                  maximal_simplitigs.add (simplitig)
149          return maximal_simplitigs
```
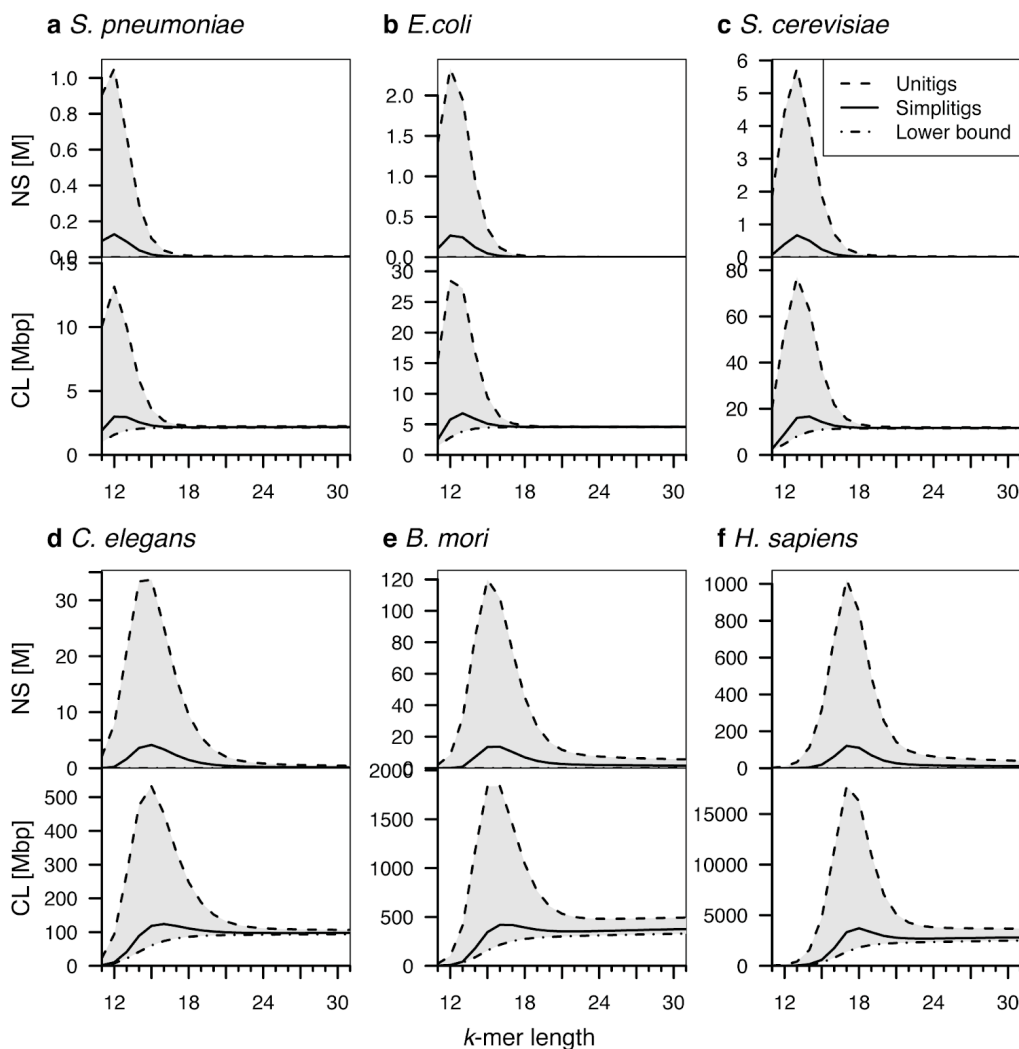
Simplitigs of model organisms

150

151 We first evaluated simplitig and unitig representations on assemblies of six model organisms (**Fig. 2**). As different

152 applications of de Bruijn graphs call for different k-mer lengths, we sought to characterize the NS and CL scaling

153 for both representations with k growing, as well as the effect of the species' genome size. Therefore, selected model

154 organisms were evaluated in an increasing order of the genome size and benchmarked for both representations on a

155 range of k-mer lengths corresponding to common alignment-free-based applications [19,20,39].

156

157 We observe that simplitigs always provide substantially better performance than unitigs (**Fig. 2**). In particular, they

158 quickly approach the theoretical lower bounds for both characteristics tested. Every data set has a range of k-mer

159 lengths where the difference between simplitigs and unitigs is very large, and after a certain threshold, the

160 difference almost vanishes. While for short genomes this threshold is located at smaller k-mer lengths than those

161 typically used in alignment-free applications (e.g., $k \approx 17$ for *E. coli*), for bigger genomes this threshold has not

162 been attained on the tested range and seems to be substantially shifted towards large k-mers (e.g., *B. mori*).

163

164 Interestingly, maxima of the NS and CL values for both representations occur very close to the value $k = log_4 G$,

165 where G is the genome size (**Fig. 2**). This is readily explained by edge saturation: for values of k up to $log_4 G$, an

166 overwhelming fraction of all 4^k k-mers belong to the genome, which makes the de Bruijn graph branch at nearly

167 every node. As a consequence, unitigs are then essentially reduced to individual k-mers and their number grows

168 exponentially whereas simplitigs stay compact on the whole range of k-mer lengths. Starting from $k = log_4 G$ the

169 graph starts to form longer non-branching paths, which drives down the NS and CL of unitigs, and they approach

170 those of simplitigs. However, the difference between simplitigs and unitigs in their count and length may stay

171 considerable even for larger values of k, especially in case of large eukaryotic genomes.

Fig. 2 Comparison of the simplitig and unitig representations for selected model organisms and a range of k-mers. The number of sequences (NS, millions) and their cumulative length (CL, megabase pairs) for both representations of six model organisms ordered by their genome size: **a** *Streptococcus pneumoniae*, 2.22 Mbp; **b** *Escherichia coli*, 4.64 Mbp; **c** *Saccharomyces cerevisiae*, 12.2 Mbp; **d** *Caenorhabditis elegans*, 100 Mbp; **e** *Bombyx mori*, 482 Mbp; and **f** *Homo sapiens*, 3.21 Gbp. The CL lower bound corresponds to the number of k-mers. Full results are available in **Additional File 1**.

8

Performance assessment

We then analyzed the computational resources that had been used to compute the simplitigs using ProphAsm and the unitigs using BCALM (**Fig. 3**). Both representations were computed in the environment of a computational cluster, with individual experiments deployed as parallel jobs using SLURM (Methods). Even though we primarily focused on the total CPU time, we also tested BCALM using 4 threads to evaluate the effect of parallelization.

We observe that throughout our experiments ProphAsm outcompeted BCALM, both in terms of the memory consumption and the CPU time, even if BCALM was run with 4 threads (**Fig. 3**). The only exception was the memory consumption for *H. sapiens*, suggesting that BCALM may be more memory-efficient for large genomes. Importantly, ProphAsm used a consistent amount of resources: memory 38–51 bytes of RAM per k-mer in the dataset, a limited CPU time and no additional disk space. On the other hand, BCALM's resource usage was less predictable and less consistent across experiments and required frequent trial-and-error resource adjustments and re-running (Methods).

Besides the comparatively high memory and CPU time requirements, the most challenging resource was the disk space. In order to fit within the available disk capacity, we reduced the BCALM consumption using the '-maxdisk' parameter. However, despite that we requested BCALM to use no more than 30 GB per experiment, a random manual inspection revealed a substantially higher use – for instance, 116 GB of disk space for *H. sapiens* with $k = 17$ and 4 threads. The extensive disk space consumption also disabled a similar comparison on a desktop computer.

Overall, the better performance of ProphAsm can be explained by simplitigs being fundamentally easier to compute than unitigs and by BCALM being optimized for a particular class of de Bruijn graphs that emerge in assembly-like applications. As the ProphAsm resource usage is highly predictable, it appears to be more suitable for the use on clusters in many parallel instances, unless the number of k-mers in the dataset exceeds a critical threshold determined by the available RAM.

205

206
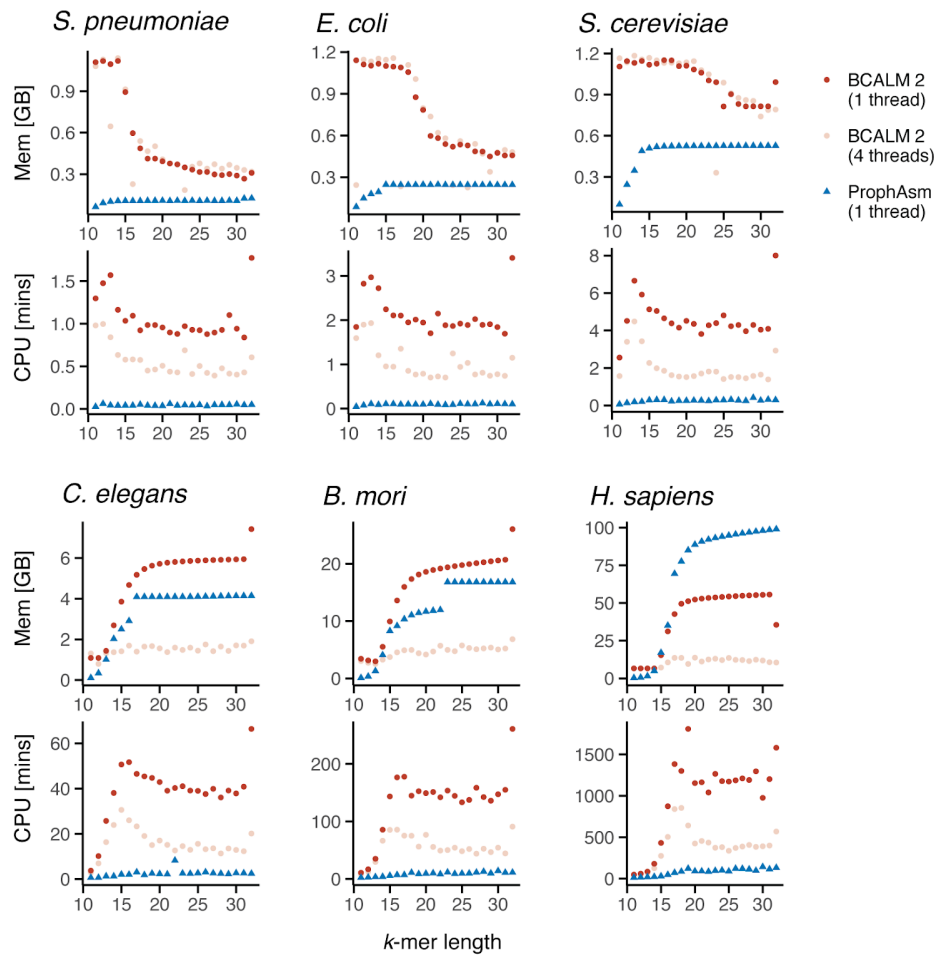
Fig. 3 Comparison of CPU time and memory consumption of ProphAsm and BCALM. Resources to compute

unitigs using BCALM (using one and four threads) and simplitigs using ProphAsm (using one thread) of the six

model organisms. Full results are available in **Additional File 2**.

Simplitigs of bacterial pan-genomes

We then sought to evaluate the impact of additional variation in a de Bruijn graph (**Fig. 4**). Such variation may originate in polymorphisms, varying gene content in a population of genomes that are represented jointly, in haplotypes of viral quasispecies, or in sequencing errors in case of graphs constructed directly from sequencing reads. In all these cases, many nodes of the de Bruijn graph become branching and new paths emerge. To model gradually increasing variation, we used bacterial pan-genomes with different levels of sampling. Given the high diversity and variability of bacteria, de Bruijn graphs provide a convenient option for computational pan-genomes [40]. Such pan-genomes can be constructed from draft assemblies or even directly from sequencing reads, and thanks to bacterial genomes being short and haploid, the information captured by the graphs is sufficient for many analyses.

We first constructed a pan-genome of *N. gonorrhoeae*, and characterized unitigs and simplitigs as a function of pan-genome size (**Fig. 4a**). We used 1,102 draft assemblies of clinical isolates from the Prevention's Gonococcal Isolate Surveillance Project [41], from which we built a series of de Bruijn graphs using an increasing number of genomes. Consistent with previous experiments (**Fig 2ab**, $k = 31$), both representations perform comparably well when only one bacterial genome is included (**Fig. 4a**). However, as the number of genomes or k-mers grows, the NS and CL grow as well, but with an increasing gap between unitigs and simplitigs; importantly, the latter stay close to the theoretical lower bounds. When the pan-genome size is measured via the number of genomes included, the CL and NS resemble logarithmic functions for both unitigs and simplitigs (**Fig. 4a**, left-hand column). However, when the number of k-mers included is used instead, the NS and CL functions act as affine functions (**Fig. 4a**, right-hand column). This suggests that a pan-genome k-mer count and a species-specific slope may be used as the predictors of simplitig performance in future applications.

To analyze the relative benefit of simplitigs with growing de Bruijn graphs, we evaluated the NS and CL reduction ratio of simplitigs over unitigs in different configurations (**Fig. 4b**). We used the same *N. gonorrhoeae* dataset and considered also another dataset of *S. pneumoniae*, consisting of 616 draft Illumina assemblies of isolates from a

236 carriage study of children in Massachusetts, USA [42,43]. For both species and for $k = 18, 31$, we constructed a

237 series of de Bruijn graphs as previously, but this time we visualized the NS and CL reduction ratios. In all cases, the

238 NS reduction ratios eventually stabilized at values close to 3, following an L-shape ($k = 18$) or being almost constant

239 ($k = 31$). The CL reduction ratio admitted approximately a logarithmic dependence on the number of genomes and

240 still resembled a linear dependence on the number of k-mers. Overall, these experiments provided further evidence

241 that the benefit of simplitigs over unitigs grows with the increased proportion of branching nodes in a de Bruijn

242 graph or with increasing data in case of pan-genome reference structures.

243

244
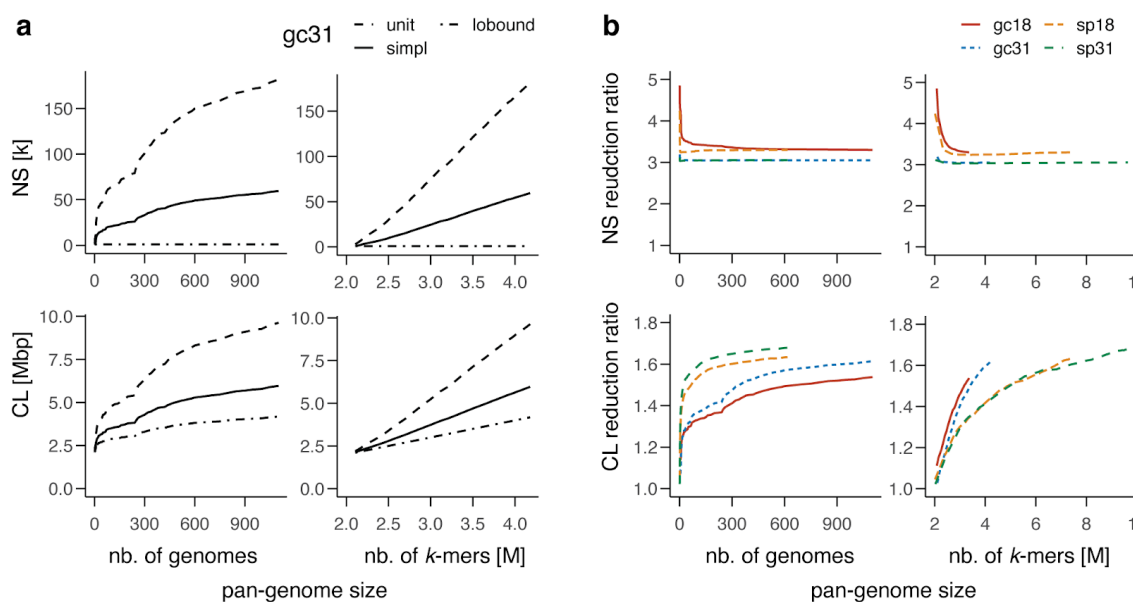
Fig. 4 Scaling of simplitigs and unitigs of bacterial pan-genomes as the pan-genome size grows with a better

sampling and more within-species variation. **a** Number of sequences (NS, thousands) and their cumulative length

(CL, megabase pairs) for simplitigs (simpl) and unitigs (unit) and the lower bound (lobound) of *N. gonorrhoeae*

and $k = 31$, as a function of the number of genomes (left) and k-mers (right, millions) included. **b** Reduction ratio

of simplitigs over unitigs for *S. pneumoniae* (sp) and *N. gonorrhoeae* (gc) and $k = 18, 31$, as a function of the

number of genomes (left) and k-mers (right, millions) included. Full results are available in **Additional File 3**.

12

Application of simplitigs for *k*-mer search

Finally, we sought to demonstrate the benefit of simplitigs in a real application. A major use of de Bruijn graphs

consists in k-mer matching, which requires the graphs to act as a membership data structure. As both simplitigs

and unitigs are text-based representations, k-mer queries can be implemented using an arbitrary full-text

index [44], notably a Burrows-Wheeler Transform index [45] (sometimes referred to as an FM-index). Here, we

used the index of BWA [46], as one of the best-engineered solutions available, to analyze the impact of unitig

replacement by simplitigs.

Single pan-genome

We first evaluated the simplitig improvement on the same *N. gonorrhoeae* pan-genome (**Fig. 5**). We considered

four different k-mer lengths $k = 19, 23, 27, 31$ and for each of them, we built three pan-genome representations from

the original draft genome assemblies: first, we merged the assemblies as the most straightforward approach to

collect all k-mers; then we computed pan-genome representations by unitigs and simplitigs. As all the three

representations carry the same k-mer set, a full-text index built upon them should provide the same results, but

with a performance reflecting the differences in NS and CL.

We analysed the NS and CL characteristics of the computed representations (**Fig. 5a**). Simplitigs improved NS and

CL over unitigs by factors of 3.1×−3.2× and 1.5×−1.6×, respectively, consistent with **Fig. 4**. This suggests that

memory required for unitigs would be approximately by 50% higher than for unitigs across all the values of k

considered. We also compared simplitigs and unitigs to assemblies; both improved the CL by two orders of

magnitude while the NS stayed comparable for simplitigs and increased twofold for unitigs.

We then evaluated k-mer query performance and memory footprint (**Fig. 5b**). For each representation, we

constructed a standard BWA index and matched 10 million random k-mers from the pan-genome using BWA

fastmap [47], with no restriction on maximum size of the suffix-array interval to ensure evaluation correctness

(Methods). Surprisingly, simplitigs improved memory by factors of 2.7× − 3.0× (**Fig. 5b**), thus twice as much as we

276 previously anticipated. This is explained by the fact that the underlying full-text engine has to keep information

277 about individual sequences in memory as separate records. As NS grows, it has a negative impact on both the

278 memory footprint and query speed. Nevertheless, since simplitigs provided a substantial reduction in NS over

279 unitigs, this overhead has been reduced. Therefore, the excessive number of unitigs observed throughout our

280 experiments (**Fig. 1** and **Fig. 2**) provides a further argument for replacing unitigs by simplitigs when possible.

281

282

283
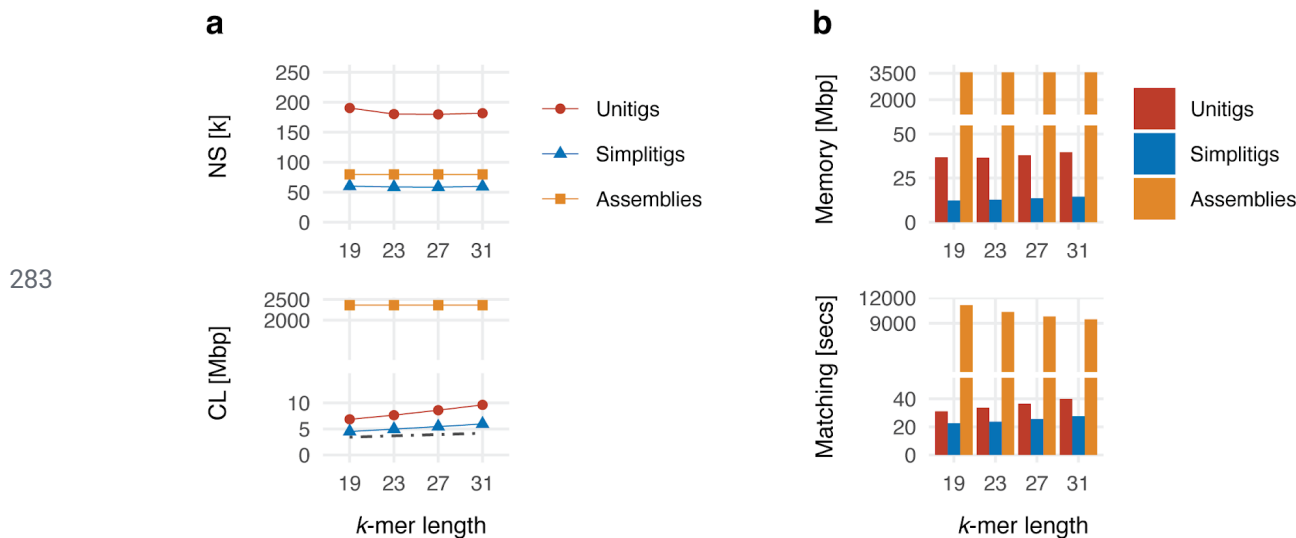
284 **Fig. 5** *K*-mer queries for the *N. gonorrhoeae* pan-genome on top of the draft assemblies, unitigs, and simplitigs.

285 **a** Characteristics of the obtained unitigs and simplitigs: number of sequences (NS, thousands) and their cumulative

286 length (CL, megabase pairs). The dot-dash line depicts the CL lower bound corresponding to the number of *k*-mers.

287 **b** Time and memory footprint of BWA *k*-mer queries (10 million *k*-mers). Full results including relative

288 improvements are available in **Additional File 4**.

14

Multiple pan-genomes

We evaluated the performance of the simplitig representation for simultaneous indexing of a large number bacterial

pan-genomes (**Fig. 6**). We downloaded all complete bacterial genomes from Genbank that had not been excluded

from RefSeq (as of May 2020; 9,869 records out of which 9,032 had genomic sequences available; Methods). We

restricted ourselves to complete genomes as draft genomes in Genbank are substantially impacted by false genetic

variability [48–50] that is particularly common in bacterial studies, mainly due to the contaminant DNA [51]. By

grouping individual genomes per species, we obtained 3,179 bacterial pan-genomes which we call the "All" dataset.

After computing simplitigs and unitigs per species, we merged the obtained representations and constructed

indexes using BWA; all this was done for $k = 19, 23, 27, 31$ to evaluate the impact of the k-mer length. As the unitig

index could not fit into RAM of our desktop computer for any k, we also created the "Solid" dataset by omitting

pan-genomes with less than 11 genomes; this resulted in 112 pan-genomes with 3,958 genomes. We provide all the

constructed pan-genomes in the form of simplitigs on Zenodo (10.5281/zenodo.3800713).

First we analyzed the obtained simplitig and unitig representations of both datasets (**Fig. 6a**). We observe that

simplitigs provide substantial improvement in both test characteristics. In the Solid dataset, NS and CL were

reduced by simplitigs by factors of 3.1–4.5 and 1.4–1.9, respectively; and in the All dataset, NS and CL were reduced

by factors of 3.0–4.3 and 1.2–1.4, respectively; all consistent with the scaling observed previously (**Fig. 4**, **Fig. 5**).

While the improvement in NS was almost identical in both datasets (consistent with the top-right graph in **Fig 4b**),

the improvement in CL was clearly better in the Solid dataset. Indeed, as the vast majority of pan-genomes in the

All dataset contained only one genome, the de Bruijn graphs had a comparatively low number of branching nodes,

therefore the difference between simplitigs and unitigs was less striking (consistent with the values for small

pan-genome sizes in **Fig 4b**). We also observe that, in contrast to unitigs, k-mer length had only little impact on

the CL of simplitigs within the tested range, which provides better guarantees on required computational resources

in future applications.

We then measured the performance of k-mer lookup (**Fig. 6b**). Both on a desktop and on a cluster, we evaluated

memory footprints, index loading time and time to match ten million random k-mers from the index using BWA

15

316 (Methods). We observed that simplitigs substantially improved the memory footprint and index loading times. For

317 $k = 19$, simplitigs largely improved the matching times, where the difference is caused by "ghost k-mers" on unitig

318 borders; these were more common in this experiment due to the short k-mer length and the high number of

319 unitigs. For higher k-mer lengths, simplitigs still provided a moderate improvement in the matching rate. We note

320 that the query time with BWT-based k-mer indexes is dominated by high-frequency k-mers. As these are equally

321 frequent in simplitigs and unitigs, the observed performance is similar unless many ghost k-mers emerge on

322 sequence borders as seen previously. On the desktop, the unitig All-index could not be evaluated as it did not fit into

323 memory, and the outlier for $k = 19$ may be the result of memory swapping.

324

325
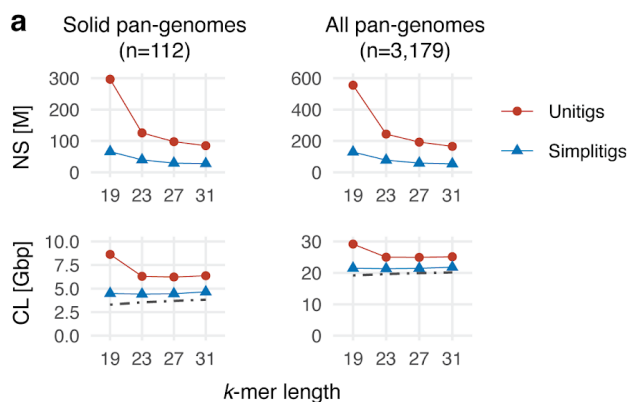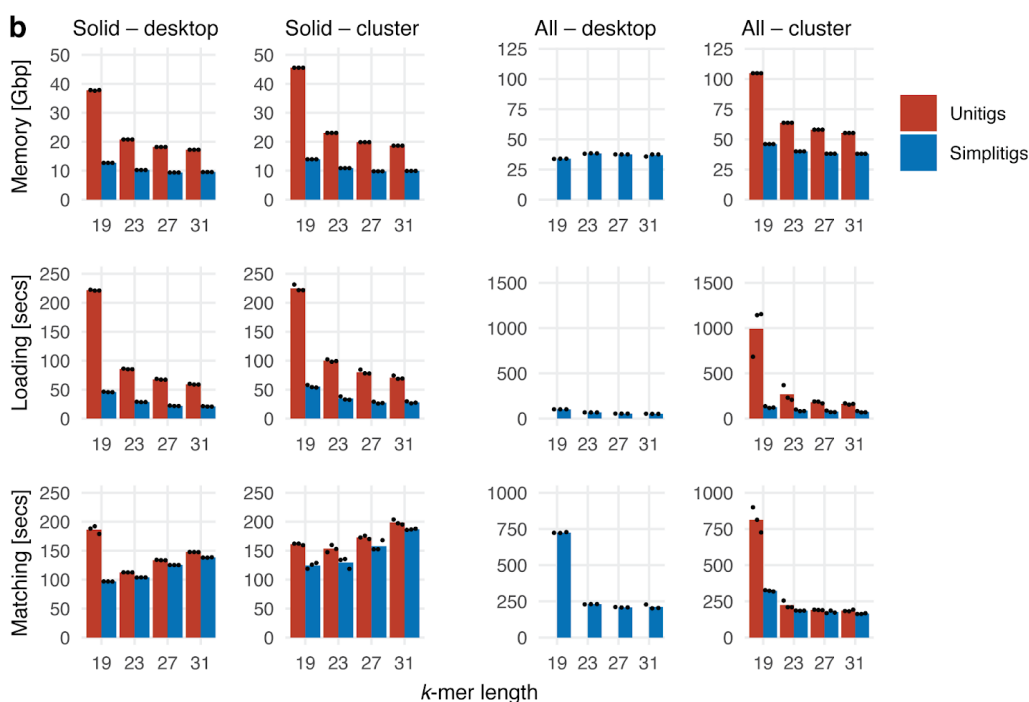
Fig. 6 K-mer queries for multiple pan-genomes indexed simultaneously. Bacterial pan-genomes were computed from the complete Genbank assemblies per individual species. While the All dataset comprises all pan-genomes with no restriction on their size, the Solid dataset comprises only those that contain at least 11 genomes. **a** Characteristics of the obtained unitigs and simplitigs: number of sequences (NS, millions) and their cumulative length (CL, gigabase pairs). The dot-dash line depicts the lower bound corresponding to the number of k-mers. **b** Memory footprint, time of index loading and time of matching 10 million k-mers using BWA. The bars correspond to the mean of three measurements (black dots). Full results including relative improvements are available in **Additional File 5**.

17

Discussion

334

We introduced the concept of simplitigs, a generalization of unitigs, and demonstrated that simplitigs constitute a

335

compact, efficient and scalable representation of de Bruijn graphs for various types of genomic datasets. The two

336

representations share many similarities: they are text-based and individual strings correspond to spellings of

337

vertex-disjoint paths. Both representations can be seen as irreversible transforms, taking a set of input strings and

338

producing a new set of strings preserving the k-mer sets. In both cases, the resulting files can easily be manipulated

339

using common Unix tools, compressed using standard compression techniques, and indexed using full-text indexes.

340

The main difference consists in that simplitigs do not explicitly carry information about the topology of the de

341

Bruijn graph. Also simplitigs are not expected to have direct biological significance – neighboring segments of the

342

same simplitig may correspond to distant parts of the same nucleic acid or even to different ones. Nevertheless,

343

unitigs can always be recomputed from simplitigs, but this step is not required for many common applications.

344

Furthermore, a concept analogous to simplitigs, called disjointigs, was recently introduced in the context of genome

345

assembly using A-Bruijn graphs [52,53], suggesting that simplitigs may be useful beyond the context of

346

topology-oblivious applications.

347

348

We provided ProphAsm, a tool implementing a greedy heuristic to efficiently compute maximal simplitigs from a k

349

-mer set. ProphAsm is a spin-off of the ProPhyle software (https://prophyle.github.io, [22,54]) for metagenomic

350

classification, allowing efficient indexing of k-mers propagated to individual nodes of a phylogenetic tree.

351

ProphAsm presents a "naive" implementation of the greedy heuristic (**Alg 1)** that can be further improved. For

352

instance, a hash table with better memory management may reduce the memory requirement by a factor of 2.5 [55].

353

Additional memory reduction may be also achieved in a similar fashion as previously done for unitigs [38,56,57].

354

Nevertheless, on the studied data, ProphAsm strikingly outcompeted BCALM in all characteristics measured, with

355

the only exception of memory in the case of *H. sapiens*.

356

357

The observed lower requirements of ProphAsm can be attributed to two major differences between unitigs and

358

simplitigs. First, unitigs, and BCALM as one of the reference programs, are designed for assembly applications,

359

18

360 where only a small proportion of nodes is usually branching. Moreover, experiments are usually run on a cluster in

361 series, with multiple threads per experiment, rather than in parallel, and the tools can use extensive disk space.

362 However, when unitigs are tested as a general representation with restricted disk space, the required resources

363 grow substantially. Second, simplitigs are likely to be, from a computational perspective, fundamentally easier than

364 unitigs.

365

366 A challenging but also promising feature of simplitig representation is the ambiguity of maximal simplitigs. This is

367 in sharp contrast to maximal unitigs, which are uniquely defined (up to the order, reverse complementing, and

368 cycles). In practice, every algorithm for simplitig computation has to decide which edge will be included at each

369 branching node. Here, we prioritized speed, simplitigs were constructed progressively and lexicographically

370 minimal edges were used in a case of ambiguity. Therefore, the final maximal simplitigs were only dependent on the

371 choice of seeding k-mers; these are determined by the specific implementation of 'std::unordered_set' in the C++

372 standard library. Nevertheless, characteristics other than speed could readily be prioritized instead. For instance, a

373 more sophisticated heuristic may shift the CL and NS closer to the optimum. One could also aim at adding

374 biological meaning to simplitigs, e.g., by preferring those paths that are better supported by sequence data. On the

375 other hand, streaming algorithms for operations such as merging or intersecting may require specific prescribed

376 forms of unitigs. Finally, simplitigs may be optimized for entropy in order to maximize their compressibility.

377

378 The data presented in this paper highlight the scaling of computational resources as more sequencing data become

379 available. The studied *N. gonorrhoeae* dataset constitutes a relatively complete image of a bacterial population in a

380 geographical region at a given time scale. As such, it can be used to model the "state of completion" of k-mer-based

381 pan-genome representations. On the other hand, the multiple pan-genomes experiment shows how simplitigs

382 perform when a large number of such pan-genomes, although in different states of completion, are considered

383 simultaneously and queried using a single BWT index. Overall, the presented experiments allow us to predict the

384 resources for species for which only limited sequence data are available at present, but more are likely to be

385 generated in the future. Importantly, with more data available, comparative benefits of simplitigs over unitigs grow

386 as we have shown throughout the paper. As the growth of public databases negatively impacts the accuracy of those

19

387 algorithms that operate on top of lossily represented de Bruijn graphs [58], simplitigs provide a promising solution

388 offering both exactness and scalability.

389

390 In modern bioinformatics applications multiple de Bruijn graphs are often considered simultaneously; the resulting

391 structure is usually referred to as a colored de Bruijn graph [14] and the associated data structures have been widely

392 studied [59–70]. Although we touched upon this setting in the Multiple pan-genomes section, exploiting the

393 similarity between individual de Bruijn graphs for further compression in simplitig-based approaches is to be

394 addressed in future work. In many applications, including some of the traditional alignment-free methods [13,71], it

395 is also desirable to consider k-mers with counts. In the context of de Bruijn graphs, this leads to the so-called

396 weighted variant of the problem [72]. The fact that frequencies of overlapping k-mers are usually similar suggests

397 that k-mers can be grouped based on frequencies and simplitigs constructed per group .

398

399 Independently and simultaneously with the work we present here, the simplitig representation was recently studied

400 in [73] under the name "spectrum-preserving string sets". The associated UST tool follows a similar greedy strategy

401 to ProphAsm, although operating on unitigs constructed by BCALM rather than on the original k-mers. As we

402 demonstrated throughout this paper, unitigs are prohibitive for highly branching de Bruijn graphs, where a

403 simplitig construction through unitigs may create a burden on resources and easily become intractable. The paper

404 presents a tighter lower bound on the cumulative length of the representation (CL), termed weight, taking into

405 account the graph topology but requiring a computational overhead. The authors also studied the compression

406 properties of simplitigs when combined with standard compression algorithms. On the other hand, the paper does

407 not study the number of sequences (NS) and continuous scaling for parameters such as k-mer length or amount of

408 additional variation included.

Conclusions

In this paper, we addressed the question of efficient and scalable representation of de Bruijn graphs. We showed that the state-of-the-art unitig representation may require adequately large computational resources, especially when de Bruijn graphs contain many branching nodes. We introduced simplitigs, which provide a more compact replacement in applications that do not require explicit information on the graph topology, such as alignment-free sequence comparison and k-mer indexing. We introduced a heuristic simplitig computation and showed on the examples of model species that unless the genome is large, even a naive implementation outperforms BCALM, the main state-of-the-art tool for unitigs. We then studied applications to bacterial pan-genomics and showed that the utility of simplitigs compared to unitigs grows as more data are available. Finally, we demonstrated on the example of full-text k-mer indexing that simplitigs can substantially reduce computational resources and allow computations in situations where unitigs would bring unaffordable costs when exactness should be preserved.

Our work opens many questions and future directions. The presented algorithm for simplitig computation can be improved, parallelized, de-randomized to ensure reproducibility. We anticipate more theoretical advances in the analysis of the minimum vertex-disjoint path cover problem and better mapping to results from other disciplines such as network sciences. We also anticipate improvements in the heuristic approaches that could simplify and parallelize simplitig computation. The nature of the algorithm suggests that simplitigs might be computed online directly from a stream of data such as sequencing reads. We anticipate better implementations and libraries for simplitigs that can be plugged into standard bioinformatics libraries for various programming languages. Another series of questions is related to low-memory transformations of computed simplitigs that would allow precomputing simplitigs on computer clusters, and tailoring to specific applications on standard computers; this includes decreasing k, performing set operations on top of simplitig sets and computing maximal unitigs from simplitigs. A substantial body of work can be anticipated in the direction of text indexing – we showed that simplitigs can be combined with full-text indexes; however, specialized simplitig indexes exploiting simplitig characteristics are yet to be developed. On the theoretical side, many perspectives are open in the direction of orthogonal algorithmic techniques, such as sketching [74,75], and in relation to other stringology concepts, such as

435 minimal absent words [76] and shortest superstrings [77]. Finally, simplitigs can serve as components in design of

436 various specialized data structures; these can involve membership queries of classes of de Bruijn graphs and colored

437 de Bruijn graphs, where simplitigs may encode not only the k-mers themselves, but also additional metadata such

438 as k-mer frequencies or colors. Furthermore, simplitigs will facilitate new full-text-based data structures for

439 approximate matching, based on the inclusion of the proximity variation, that would be completely intractable with

440 unitigs. Overall, we anticipate that the simplitig representation will become a generic compact representation of de

441 Bruijn graphs, in particular, in the context of large-scale sequence data search engines [69] and sequence data

442 repositories such as those of NCBI and EBI.

Methods

De Bruijn graphs

All strings are assumed to be over the alphabet $\{A,C,G,T\}$. A k-mer is a string of length k. For a string $s = s_1...s_n$,

we define $pref_k(s) = s_1 \cdots s_k$ and $suf_k(s) = s_{n-k+1} \cdots s_n$. For two strings s and t of length at least k, we define the

binary connectivity relation $s \rightarrow_k t$ if and only if $suf_k(s) = pref_k(t)$. If $s \rightarrow_k t$, we define the k-merging operation $\odot$ as

$s \odot^k t = s \cdot suf_{|t|-k}(t)$.

Given a set K of k-mers, the *de Bruijn graph* of K is the directed graph $G = (V,E)$ with $V = K$ and

$E = \{(u,v) \in K^2 \mid u \rightarrow_{k-1} v\}$. For every path $p = (v_1,...,v_p)$ in G, the string $v_1 \odot^{k-1} v_2 \odot^{k-1} ... \odot^{k-1} v_p$ is called a *spelling* of

p. This definition of de Bruijn graphs is *node-centric*, as nodes are identified with k-mers and edges are implicit.

Therefore, we can use the terms "k-mer set" and "de Bruijn graph" interchangeably.

Simplitigs

Consider a set K of k-mers and the corresponding de Bruijn graph $G = (K,E)$. A *simplitig graph* $G' = (K,E')$ is a

spanning subgraph of G that is acyclic and the in-degree and out-degree of any node is at most one. It follows from

this definition that a simplitig graph is a vertex-disjoint union of paths, whose spellings we call *simplitigs*. A

simplitig is called *maximal* if it cannot be extended forward or backward without breaking the definition of

simplitig graph. In more detail, a simplitig $u_1 \rightarrow_{k-1} u_2 \rightarrow_{k-1} ... \rightarrow_{k-1} u_n$ is maximal if the following conditions hold

- either u_1 has no incoming edges in G, or for any edge $(v,u_1) \in E$, v belongs to another simplitig and it is
  not its last vertex,
- either u_n has no outgoing edges in G, or for any edge $(u_n,v) \in E$, v belongs to another simplitig and it is
  not its first vertex.

A *unitig* is a simplitig $u_1 \rightarrow_{k-1} u_2 \rightarrow_{k-1} ... \rightarrow_{k-1} u_n$ such that each of the nodes $u_2,...,u_n$ has in-degree 1 and each of the

nodes $u_1,...,u_{n-1}$ has out-degree 1 in graph G. A maximal unitig is defined similarly.

Comparing simplitig and unitig representations

Simplitigs and unitigs representations were compared in terms of the number of sequences produced (NS) and their cumulative length (CL). For any set of simplitigs (i.e., not necessarily maximal ones), NS is bounded by 1 and $\#kmers$, CL is bounded by $\#kmers$ and $k \cdot \#kmers$. The upper bound corresponds to the state of maximal fragmentation, where every k-mer forms a simplig. The lower bound corresponds to the maximum possible degree of compaction, i.e., a single simplitig containing all k-mers.

NS and CL are readily connected by the following formula:

$$CL = \#kmers + (k-1) \cdot NS \qquad \text{(eq 1)}$$

As an important consequence, both characteristics are optimized simultaneously.

Greedy computation of simplitigs

The problem of computing maximal simplitigs that are optimal in CL (i.e., also in NS) corresponds to the minimum vertex-disjoint path cover problem [78]. This is known to be NP-hard in the general case, reducing from the Hamiltonian path problem. However, the complexity for de Bruijn graphs remains an open question. A greedy heuristic to compute maximal simplitigs has been used throughout this paper (**Alg. 1**). Simplitigs are constructed iteratively, starting from (arbitrary) seeding k-mers and being extended greedily forwards and backwards as long as possible.

ProphAsm implementation

ProphAsm is written in C++ and implements the greedy approach described above (**Alg. 1**). K-mers are encoded using uint64_t and stored in an std::unordered_map. The choice of extension nucleotides on branching nodes is done based on the lexicographic order. Therefore, the only source of randomness is the choice of seeding k-mers by std::unordered_set::begin; the C++ standard library makes no guarantees on which specific element is considered the first element. ProphAsm does not require any disk space to store intermediate data and its memory

489 consumption corresponded to 38–51 bytes per a unique k-mer (in dependence on the allocation), consistent with

490 [55].

Uni-directed and bi-directed models

492 The uni-directed model, as presented above, is useful for introducing the concepts of unitigs and simplitigs, but is

493 not directly applicable to data obtained using sequencing: since DNA is double-stranded, every string may come

494 from either strand. At the level of k-mers, double-strandedness can be accounted for by using canonical k-mers,

495 i.e., by pairing-up every k-mer with its reverse complement, typically done by taking the lexicographical minimum

496 of the k-mer and its reverse complement. This subsequently requires redefinining de Bruijn graphs to bi-directed

497 de Bruijn graphs [79], which requires a more complex formalism.

Correctness evaluation

499 The correctness of simplitig computation can be verified using an arbitrary k-mer counter. Simplitigs have been

500 computed correctly if and only if every k-mer is present exactly once and the number of distinct k-mers is the same

501 as in the original datasets. The correctness of ProphAsm outputs was verified using JellyFish 2 [29].

Experimental evaluation – model organisms and performance

503 Reference sequences for six selected model organisms were downloaded from RefSeq and UCSC Genome Browser:

504 *S. pneumoniae* str. ATCC 700669 (accession: NC_011900.1, length 2.22 Mbp), *E. coli* str. K-12 (accession:

505 NC_000913.3, length: 4.64 Mbp), *S. cerevisiae* (accession: NC_001133.9, length: 12.2 Mbp), *C. elegans* (accession:

506 GCF_000002985.6, length: 100 Mbp), *B. mori* (accession: GCF_000151625.1, length: 482 Mbp), and *H. sapiens*

507 (HG38, http://hgdownload.soe.ucsc.edu/goldenPath/hg38/bigZips/hg38.fa.gz, length: 3.21 Gbp). For each

508 genome, simplitigs and unitigs were computed using ProphAsm and BCALM, respectively, for a range of k-mer

509 lengths [11,31].

510

511 Individual experiments were run in parallel on the Harvard Medical School O2 cluster using Snakemake [80] and

512 SLURM. ProphAsm and BCALM were run with the following parameters, respectively: '-k {kmer-length}' and

25

513 '-kmer-size {kmer-length} -abundance-min 1 -nb-cores {cores} -max-disk 30000'. As BCALM requires a large

514 undocumented amount of disk space, we used the -max-disk parameter to make a parallel execution of many

515 BCALM jobs feasible. The SLURM specifications of resource allocation for individual species were iteratively

516 adjusted until all jobs would finish; the final required resources are provided in **Supplementary Table 1**. Time

517 and memory consumption of jobs were measured independently using GNU Time. Individual jobs were deployed to

518 computational nodes with different hardware configurations, which are specified in **Additional File 2**.

519

520 **Supplementary Table 1** SLURM resource allocation for ProphAsm and BCALM2 for the performance evaluation.

Species	ProphAsm (1 core)		BCALM (1 core)		BCALM (4 cores)	
	mem [GB]	cpu [hours]	mem [GB]	cpu [hours]	mem [GB]	cpu [hours]
S. pneumoniae	10	1	10	1	10	1
E. coli	10	1	10	1	10	1
S. cerevisiae	10	1	10	1	10	1
C. elegans	10	1	10	2	10	2
B. mori	20	2	30	10	30	2
H. sapiens	120	4	100	48	100	18

521

Experimental evaluation – bacterial pan-genomes

523 First, 1,102 draft assemblies of *N. gonorrhoeae* clinical isolates (collected from 2000 to 2013 by the Centers for

524 Disease Control and Prevention's Gonococcal Isolate Surveillance Project [41], and sequenced using Illumina

525 HiSeq) were downloaded from Zenodo [81]. Second, 616 draft assemblies of *S. pneumoniae* isolates (collected from

526 2001 to 2007 for a carriage study of children in Massachusetts, USA [42,43], and sequenced using Illumina HiSeq)

527 were downloaded from the SRA FTP server using the accession codes provided in Table 1 in [43]. For each of these

528 datasets, an increasing number of genomes was being taken and merged, and simplitigs and unitigs computed using

529 ProphAsm and BCALM, respectively. This experiment was performed for $k = 18$ and $k = 31$. To avoid excessive

530 resource usage the functions were evaluated at selected points in an increasing distance: for intervals [10, 100] and

531 [100,+∞] only multiples of 5 and 20 were evaluated, respectively.

26

Experimental evaluation – full-text *k*-mer queries

532

533 In the single pan-genome experiment, the same 1,102 assemblies of *N. gonorrhoeae* were merged into a single file.

534 ProphAsm and BCALM were then used to compute simplitigs and unitigs, respectively, from this file for

535 $k = 19, 23, 27, 31$. Each of the three obtained FASTA files (assemblies, simplitigs, and unitigs) was used to

536 construct a BWA index, which was then queried for k-mers using 'bwa fastmap -l {kmer-length}'. We used a

537 modified version of BWA fastmap that reports both the time of index loading and the time of querying

538 (http://github.com/karel-brinda/bwa, commit e1f907c). Query k-mers were generated from the same pan-genome

539 using WGsim (version 1.10, with the parameters '-h 0 -S 42 -r 0.0 -1 {kmer-length} -N 10000000 -e 0').

540

541 For the multiple pan-genome experiment, a list of available bacterial assemblies was downloaded from

542 ftp://ftp.ncbi.nlm.nih.gov/genomes/genbank/bacteria/assembly_summary.txt (2020/05/05). For all assemblies

543 marked as complete (i.e., the "assembly_level" column equal to "Complete genome") and present in RefSeq (i.e., an

544 empty value in the column "excluded_from_refseq"), directory urls and species names were extracted (n=9,869).

545 These were then used to download the genomes of the isolates using RSync, restricting to genomic sequences only

546 (i.e., files matching '*v?_genomic.fna.gz', n=9,032). The downloaded assemblies were then merged per species in

547 order to collect k-mers of individual pan-genomes and used for computing simplitigs and unitigs using ProphAsm

548 and BCALM, respectively. The obtained simplitig and unitig files were then merged per categories (e.g., simplitigs

549 for k=19) and used to construct a BWA index. The obtained indexes were queried for 10 million k-mers using BWA

550 fastmap as previously. The k-mers were generated from the original assemblies of randomly selected 100 genomes

551 using DWGsim [82] (version 0.1.11, with the parameters '-R 0 -e 0 -r 0 -X 0 -y 0 -H -z 42 -m /dev/null -N

552 10000000 -1 {k} -2 0'); the randomization was performed using 'sort -R'.

553

Computational setup

554

555 The experiments were performed on the HMS O2 research high-performance cluster and on an iMac 4.2 GHz

556 Quad-Core Intel Core i7 with 40 GB RAM. The reproducibility of computation was ensured using BioConda [83].

557 All benchmarking was performed using ProphAsm 0.1.1 (commit ea28b708) and BCALM 2.2.2 (commit febf79a3).

558 Time and memory footprint were measured using GNU Time.

Declarations

Ethics approval and consent to participate

Not applicable.

Availability of data and materials

Additional files

Additional File 1. Detailed information for the single genome experiment: NS, CL and #kmers for unitigs and simplitigs as a function of k for the 6 species: **a** *S. pneumoniae*, **b** *E. coli*, **c** *S. cerevisiae*, **d** *C. elegans*, **e** *B. mori*, and **f** *H. sapiens*.

Additional File 2. Detailed information for the performance comparison. **a** CPU time and memory consumption (both measured by GNU Time and Snakemake) as a function of species, method, number of threads, and k-mer length, including the used computational node. **b** Hardware specifications for individual computational nodes.

Additional File 3. Detailed information for the pan-genome scaling experiment: **a** *N. gonorrhoeae*, $k = 18$; **b** *N. gonorrhoeae*, $k = 31$; **c** *S. pneumoniae*, $k = 18$; **d** *S. pneumoniae*, $k = 31$.

Additional File 4. Detailed information for the single pan-genome k-mer indexing experiment. **a** Characteristics of the resulting simplitigs and unitigs for $k = 19, 23, 27, 31$. **b** Memory footprint, index loading time and time to query 10 million k-mers using BWA.

Additional File 5. Detailed information for the multiple pan-genomes k-mer indexing experiment. **a** List of all genomes used for building the pan-genomes (accession code, version, species, filename, number of sequences, genome size [bp]); **b** List of species and the number of genomes included. **c** Characteristics of the resulting simplitigs and unitigs of individual pan-genomes for $k = 19, 23, 27, 31$. **d** Characteristics of the resulting simplitigs and unitigs for the All-dataset and Solid-dataset and $k = 19, 23, 27, 31$. **e** Memory footprint, index loading time and time to query 10 million k-mers using BWA (individual repetitions).

Data

All data generated or analysed during this study are included in this published article and its supplementary

information files. The simplitigs of the Human genome (HG38, for $k = 10, 11, ..., 32$) and the obtained Genbank

pan-genomes (for $k = 19, 23, 27, 31$) are provided on Zenodo under the accessions 10.5281/zenodo.3770419 and

10.5281/zenodo.3800713, respectively. The code used for the analyses is provided on Github

(https://github.com/karel-brinda/simplitigs-supplementary).

Software

ProphAsm is open source, licensed under the MIT License. The program was developed in C++ and its source code

is available from Github (http://github.com/prophyle/prophasm). ProphAsm binaries for Linux and OS X are

distributed through BioConda [83] (https://bioconda.github.io/recipes/prophasm/README.html). The source

code of the version used in this paper was deposited in Zenodo (10.5281/zenodo.3887035).

Competing interests

No competing interests.

Funding

Authors' contributions

KB, MB, GK designed the study, contributed to interpretation of the results, wrote the manuscript, and approved

the final manuscript. KB developed the software and performed the data analysis. KB and GK developed the theory.
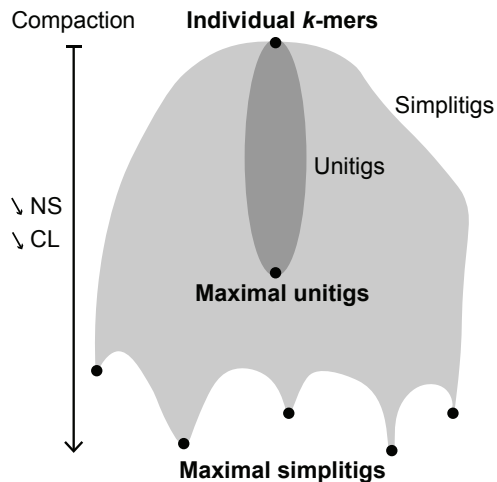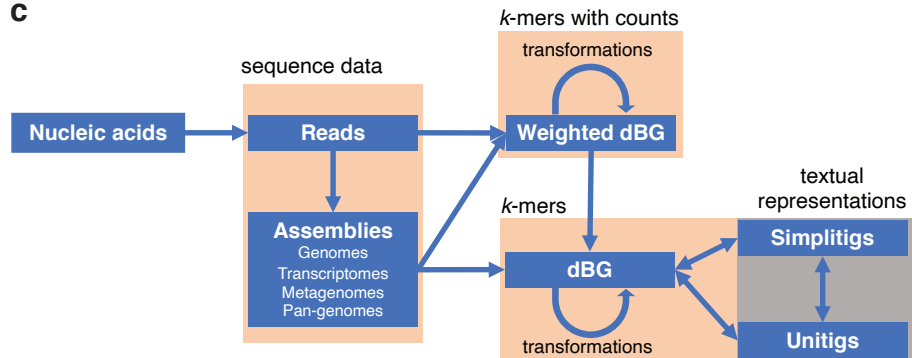
Acknowledgements

References

607 1. Needleman SB, Wunsch CD. A general method applicable to the search for similarities in the amino acid sequence
608 of two proteins. J Mol Biol. 1970;48:443–53.

609 2. Smith TF, Waterman MS. Identification of common molecular subsequences. J Mol Biol. 1981;147:195–7.

610 3. Gotoh O. An improved algorithm for matching biological sequences. J Mol Biol. 1982;162:705–8.

611 4. Idury RM, Waterman MS. A New Algorithm for DNA Sequence Assembly. J Comput Biol. 1995;2:291–306.

612 5. Pevzner PA. 1-Tuple DNA Sequencing: Computer Analysis. J Biomol Struct Dyn. 1989;7:63–73.

613 6. Pevzner PA, Tang H, Waterman MS. An Eulerian path approach to DNA fragment assembly. Proceedings of the
614 National Academy of Sciences. 2001;98:9748–53.

615 7. Zerbino DR, Birney E. Velvet: algorithms for de novo short read assembly using de Bruijn graphs. Genome Res.
616 2008;18:821–9.

617 8. Simpson JT, Wong K, Jackman SD, Schein JE, Jones SJM. ABySS: A parallel assembler for short read sequence
618 data. 2009;1117–23.

619 9. Bankevich A, Nurk S, Antipov D, Gurevich A a., Dvorkin M, Kulikov AS, et al. SPAdes: A New Genome Assembly
620 Algorithm and Its Applications to Single-Cell Sequencing. J Comput Biol. 2012;19:455–77.

621 10. Chikhi R, Rizk G. Space-efficient and exact de Bruijn graph representation based on a Bloom filter. Algorithms
622 Mol Biol. 2013;8:22.

623 11. Li D, Liu C-M, Luo R, Sadakane K, Lam T-W. MEGAHIT: an ultra-fast single-node solution for large and
624 complex metagenomics assembly via succinct de Bruijn graph. Bioinformatics. 2015;31:1674–6.

625 12. Souvorov A, Agarwala R, Lipman DJ. SKESA: strategic k-mer extension for scrupulous assemblies. Genome
626 Biol. 2018;19:153.

627 13. Zielezinski A, Vinga S, Almeida J, Karlowski WM. Alignment-free sequence comparison: benefits, applications,
628 and tools. Genome Biol. 2017;18:186.

629 14. Iqbal Z, Caccamo M, Turner I, Flicek P, McVean G. De novo assembly and genotyping of variants using colored
630 de Bruijn graphs. Nat Genet. 2012;44:226–32.

631 15. Bradley P, Gordon NC, Walker TM, Dunn L, Heys S, Huang B, et al. Rapid antibiotic-resistance predictions from
632 genome sequence data for Staphylococcus aureus and Mycobacterium tuberculosis. Nat Commun. Nature
633 Publishing Group; 2015;6:10063.

634 16. Shajii AR, Yorukoglu D, William Yu Y, Berger B, Yu YW, Berger B. Fast genotyping of known SNPs through
635 approximate k-mer matching. Bioinformatics. 2016;32:i538–44.

636 17. Sun C, Medvedev P. Toward fast and accurate SNP genotyping from whole genome sequencing data for bedside
637 diagnostics. Bioinformatics. 2019;35:415–20.

638 18. Nordström KJV, Albani MC, James GV, Gutjahr C, Hartwig B, Turck F, et al. Mutation identification by direct
639 comparison of whole-genome sequencing data from mutant and wild-type individuals using k-mers. Nat
640 Biotechnol. 2013;31:325–30.

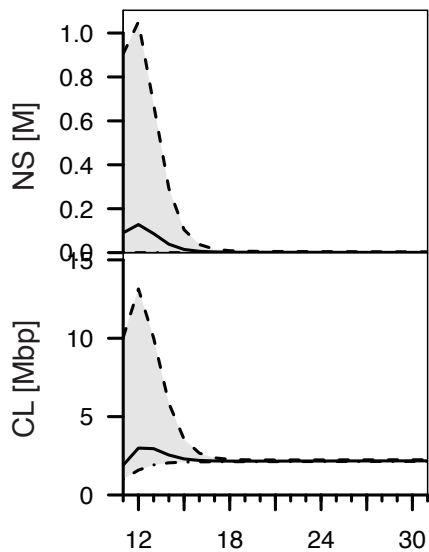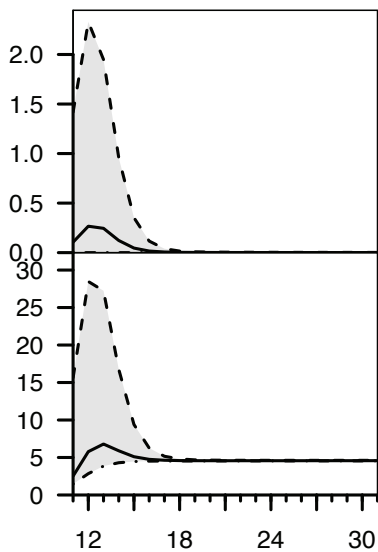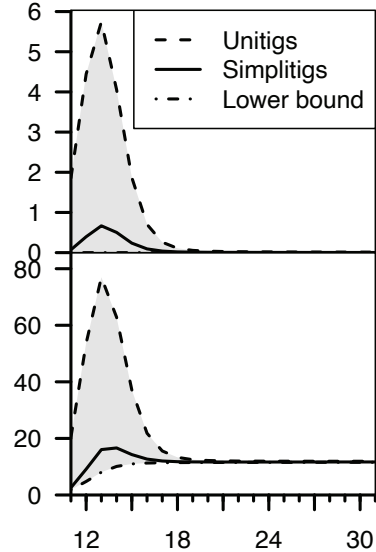641 19. Bray NL, Pimentel H, Melsted P, Pachter L. Near-optimal probabilistic RNA-seq quantification. Nat Biotechnol.

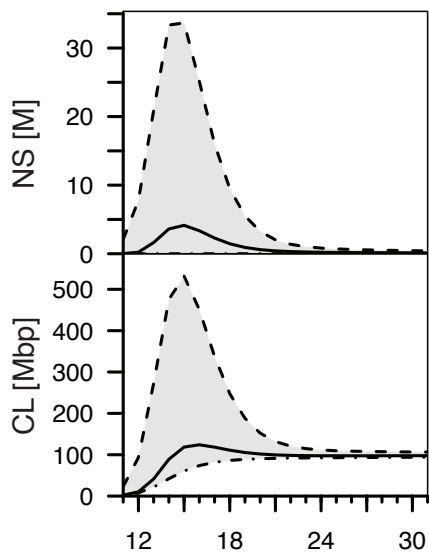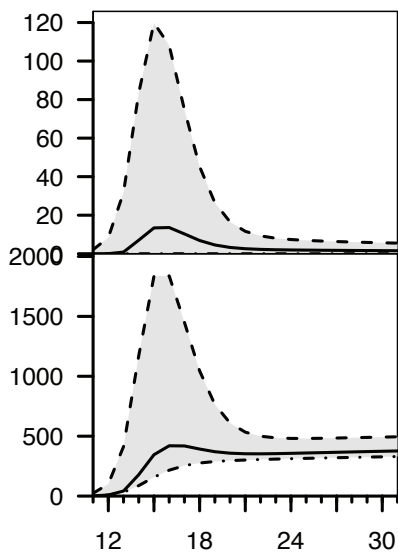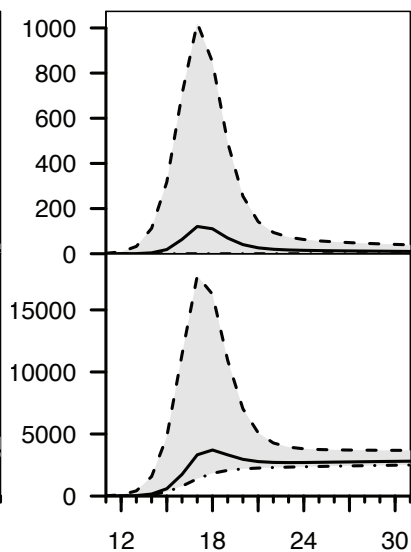642 2016;34:525–7.

643 20. Wood DE, Salzberg SL. Kraken: ultrafast metagenomic sequence classification using exact alignments. Genome
644 Biol. 2014;15:R46.

645 21. Ames SK, Hysom DA, Gardner SN, Lloyd GS, Gokhale MB, Allen JE. Scalable metagenomic taxonomy
646 classification using a reference genome database. Bioinformatics. 2013;29:2253–60.

647 22. Břinda K, Salikhov K, Pignotti S, Kucherov G. ProPhyle: An accurate, resource-frugal and deterministic DNA
648 sequence classifier [Internet]. Zenodo; 2017. Available from: https://zenodo.org/record/1054443

649 23. Corvelo A, Clarke WE, Robine N, Zody MC. taxMaps: comprehensive and highly accurate taxonomic
650 classification of short-read data in reasonable time. Genome Res. 2018;28:751–8.

651 24. Ye SH, Siddle KJ, Park DJ, Sabeti PC. Benchmarking Metagenomics Tools for Taxonomic Classification. Cell.
652 Elsevier Inc.; 2019;178:779–94.

653 25. Paten B, Novak AM, Eizenga JM, Garrison E. Genome graphs and the evolution of genome inference. Genome
654 Res. 2017;27:665–76.

655 26. Sirén J. Indexing Variation Graphs. 2017 Proceedings of the Ninteenth Workshop on Algorithm Engineering
656 and Experiments (ALENEX). Philadelphia, PA: Society for Industrial and Applied Mathematics; 2017. p. 13–27.

657 27. Garrison E, Sirén J, Novak AM, Hickey G, Eizenga JM, Dawson ET, et al. Variation graph toolkit improves read
658 mapping by representing genetic variation in the reference. Nat Biotechnol. Nature Publishing Group;
659 2018;36:875–81.

660 28. Melsted P, Pritchard JK. Efficient counting of k-mers in DNA sequences using a bloom filter. BMC
661 Bioinformatics. BioMed Central Ltd; 2011;12:333.

662 29. Marçais G, Kingsford C. A fast, lock-free approach for efficient parallel counting of occurrences of k-mers.
663 Bioinformatics. 2011;27:764–70.

664 30. Deorowicz S, Debudaj-Grabysz A, Grabowski S. Disk-based k-mer counting on a PC. BMC Bioinformatics.
665 2013;14:160.

666 31. Rizk G, Lavenier D, Chikhi R. DSK: k-mer counting with very low memory usage. Bioinformatics.
667 2013;29:652–3.

668 32. Roy RS, Bhattacharya D, Schliep A. Turtle: Identifying frequent k-mers with cache-efficient algorithms.
669 Bioinformatics. 2014;30:1950–7.

670 33. Crusoe MR, Alameldin HF, Awad S, Boucher E, Caldwell A, Cartwright R, et al. The khmer software package:
671 enabling efficient nucleotide sequence analysis. F1000Res. 2015;1–12.

672 34. Deorowicz S, Kokot M, Grabowski S, Debudaj-Grabysz A. KMC 2: fast and resource-frugal k-mer counting.
673 Bioinformatics. 2015;31:1569–76.

674 35. Kokot M, Dlugosz M, Deorowicz S. KMC 3: counting and manipulating k-mer statistics. Bioinformatics.
675 2017;33:2759–61.

676 36. Pandey P, Bender MA, Johnson R, Patro R, Berger B. Squeakr: an exact and approximate k-mer counting
677 system. Bioinformatics. 2018;34:568–75.

678 37. Chikhi R, Limasset A, Jackman S, Simpson JT, Medvedev P. On the Representation of De Bruijn Graphs. J
679 Comput Biol. 2015;22:336–52.

680 38. Chikhi R, Limasset A, Medvedev P. Compacting de Bruijn graphs from sequencing data quickly and in low

681 memory. Bioinformatics. 2016;32:i201–8.

682 39. Břinda K, Callendrello A, Ma KC, MacFadden DR, Charalampous T, Lee RS, et al. Rapid inference of antibiotic
683 resistance and susceptibility by genomic neighbour typing. Nature Microbiology [Internet]. 2020; Available from:
684 http://dx.doi.org/10.1038/s41564-019-0656-6

685 40. Marschall T, Marz M, Abeel T, Dijkstra L, Dutilh BE, Ghaffaari A, et al. Computational pan-genomics: status,
686 promises and challenges. Brief Bioinform. 2016;184:bbw089.

687 41. Grad YH, Harris SR, Kirkcaldy RD, Green AG, Marks DS, Bentley SD, et al. Genomic Epidemiology of
688 Gonococcal Resistance to Extended-Spectrum Cephalosporins, Macrolides, and Fluoroquinolones in the United
689 States, 2000–2013. J Infect Dis. 2016;214:1579–87.

690 42. Croucher NJ, Finkelstein JA, Pelton SI, Mitchell PK, Lee GM, Parkhill J, et al. Population genomics of
691 post-vaccine changes in pneumococcal epidemiology. Nat Genet. Nature Publishing Group; 2013;45:656–63.

692 43. Croucher NJ, Finkelstein JA, Pelton SI, Parkhill J, Bentley SD, Lipsitch M, et al. Population genomic datasets
693 describing the post-vaccine evolutionary epidemiology of Streptococcus pneumoniae. Scientific data.
694 2015;2:150058.

695 44. Mäkinen V, Belazzougui D, Cunial F, Tomescu AI. Genome-Scale Algorithm Design. Cambridge University
696 Press; 2015.

697 45. Ferragina P, Manzini G. Opportunistic data structures with applications. Proceedings 41st Annual Symposium
698 on Foundations of Computer Science. IEEE Comput. Soc; 2000. p. 390–8.

699 46. Li H, Durbin R. Fast and accurate short read alignment with Burrows–Wheeler transform. Bioinformatics.
700 Narnia; 2009;25:1754–60.

701 47. Li H. Exploring single-sample SNP and INDEL calling with whole-genome de novo assembly. Bioinformatics.
702 2012;28:1838–44.

703 48. Merchant S, Wood DE, Salzberg SL. Unexpected cross-species contamination in genome sequencing projects.
704 PeerJ. 2014;2:e675.

705 49. Lu J, Salzberg SL. Removing contaminants from databases of draft genomes. PLoS Comput Biol.
706 2018;14:e1006277.

707 50. Steinegger M, Salzberg SL. Terminating contamination: large-scale search identifies more than 2,000,000
708 contaminated entries in GenBank [Internet]. bioRxiv. 2020. p. 2020.01.26.920173. Available from:
709 https://www.biorxiv.org/content/10.1101/2020.01.26.920173v1

710 51. Goig GA, Blanco S, Garcia-Basteiro AL, Comas I. Contaminant DNA in bacterial sequencing experiments is a
711 major source of false genetic variability. BMC Biol. 2020;18:24.

712 52. Lin Y, Yuan J, Kolmogorov M, Shen MW, Chaisson M, Pevzner PA. Assembly of long error-prone reads using de
713 Bruijn graphs. Proc Natl Acad Sci U S A. 2016;113:E8396–405.

714 53. Kolmogorov M, Yuan J, Lin Y, Pevzner PA. Assembly of long, error-prone reads using repeat graphs. Nat
715 Biotechnol. 2019;37:540–6.

716 54. Břinda K. Novel computational techniques for mapping and classification of Next-Generation Sequencing data
717 [Internet]. 2016. Available from: https://hal.archives-ouvertes.fr/tel-01484198/

718 55. Li H. Revisiting hash table performance [Internet]. Attractive Chaos. 2018 [cited 2020 May 1]. Available from:
719 https://attractivechaos.wordpress.com/2018/01/13/revisiting-hash-table-performance/

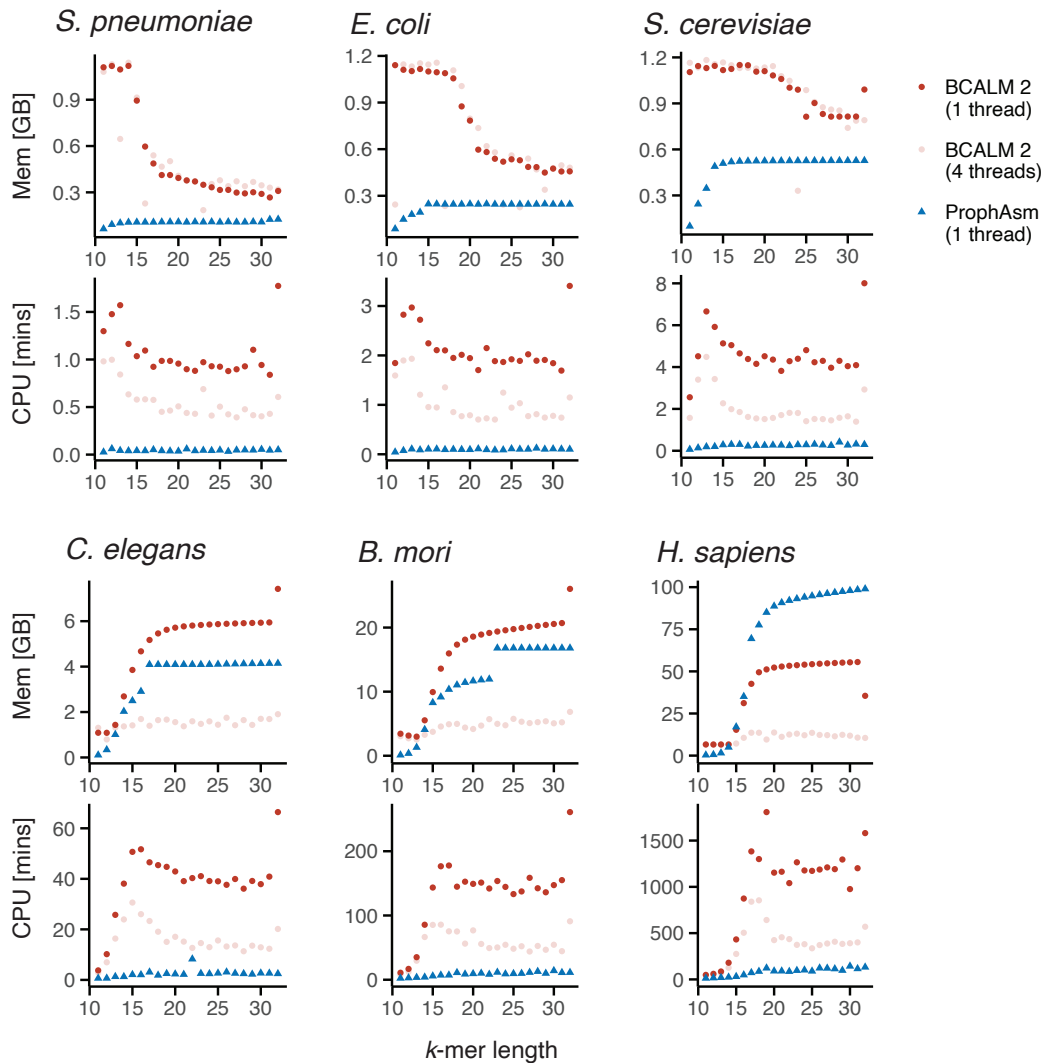720 56. Pan T, Nihalani R, Aluru S. Fast de Bruijn Graph Compaction in Distributed Memory Environments.

721 IEEE/ACM Trans Comput Biol Bioinform. 2018;1–1.

722 57. Guo H, Fu Y, Gao Y, Li J, Wang Y, Liu B. deGSM: memory scalable construction of large scale de Bruijn Graph.
723 IEEE/ACM Trans Comput Biol Bioinform. 2019;1–1.

724 58. Nasko DJ, Koren S, Phillippy AM, Treangen TJ. RefSeq database growth influences the accuracy of k-mer-based
725 lowest common ancestor species identification. Genome Biol. 2018;19:165.

726 59. Bowe A, Onodera T, Sadakane K, Shibuya T. Succinct de Bruijn Graphs. In: Raphael B, Tang J, editors.
727 Algorithms in Bioinformatics. Berlin, Heidelberg: Springer Berlin Heidelberg; 2012. p. 225–35.

728 60. Holley G, Wittler R, Stoye J. Bloom Filter Trie: an alignment-free and reference-free data structure for
729 pan-genome storage. Algorithms Mol Biol. BioMed Central; 2016;11:3.

730 61. Solomon B, Kingsford C. Fast search of thousands of short-read sequencing experiments. Nat Biotechnol.
731 2016;34:300–2.

732 62. Muggli MD, Bowe A, Noyes NR, Morley PS, Belk KE, Raymond R, et al. Succinct colored de Bruijn graphs.
733 Bioinformatics. 2017;33:3181–7.

734 63. Sun C, Harris RS, Chikhi R, Medvedev P. AllSome Sequence Bloom Trees. J Comput Biol. 2018;25:467–79.

735 64. Pandey P, Almodaresi F, Bender MA, Ferdman M, Johnson R, Patro R. Mantis: A Fast, Small, and Exact
736 Large-Scale Sequence-Search Index. Cell Syst. 2018;7:201–7.e4.

737 65. Yu Y, Liu J, Liu X, Zhang Y, Magner E, Lehnert E, et al. SeqOthello: querying RNA-seq experiments at scale.
738 Genome Biol. 2018;19:167.

739 66. Almodaresi F, Sarkar H, Srivastava A, Patro R. A space and time-efficient index for the compacted colored de
740 Bruijn graph [Internet]. Bioinformatics. 2018. p. i169–77. Available from:
741 http://dx.doi.org/10.1093/bioinformatics/bty292

742 67. Harris RS, Medvedev P. Improved representation of sequence Bloom trees [Internet]. Bioinformatics. 2019.
743 Available from: http://dx.doi.org/10.1093/bioinformatics/btz662

744 68. Holley G, Melsted P. Bifrost – Highly parallel construction and indexing of colored and compacted de Bruijn
745 graphs [Internet]. bioRxiv. 2019. p. 695338. Available from: https://www.biorxiv.org/content/10.1101/695338v2

746 69. Bradley P, den Bakker HC, Rocha EPC, McVean G, Iqbal Z. Ultrafast search of all deposited bacterial and viral
747 genomic data. Nat Biotechnol. Springer US; 2019;37:152–9.

748 70. Bingmann T, Bradley P, Gauger F, Iqbal Z. COBS: A Compact Bit-Sliced Signature Index. String Processing and
749 Information Retrieval. Springer International Publishing; 2019. p. 285–303.

750 71. Zielezinski A, Girgis HZ, Bernard G, Leimeister C-A, Tang K, Dencker T, et al. Benchmarking of alignment-free
751 sequence comparison methods. Genome Biol. 2019;20:144.

752 72. Pandey P, Bender MA, Johnson R, Patro R. deBGR: an efficient and near-exact representation of the weighted
753 de Bruijn graph. Bioinformatics. 2017;33:i133–41.

754 73. Rahman A, Medvedev P. Representation of k-mer sets using spectrum-preserving string sets [Internet]. bioRxiv.
755 2020 [cited 2020 Jan 20]. p. 2020.01.07.896928. Available from:
756 https://www.biorxiv.org/content/10.1101/2020.01.07.896928v1.abstract

757 74. Rowe WPM. When the levee breaks: a practical guide to sketching algorithms for processing the flood of
758 genomic data. Genome Biol. Genome Biology; 2019;20:199.

759 75. Elworth RAL, Wang Q, Kota PK, Barberan CJ, Coleman B, Balaji A, et al. To Petabytes and beyond: recent
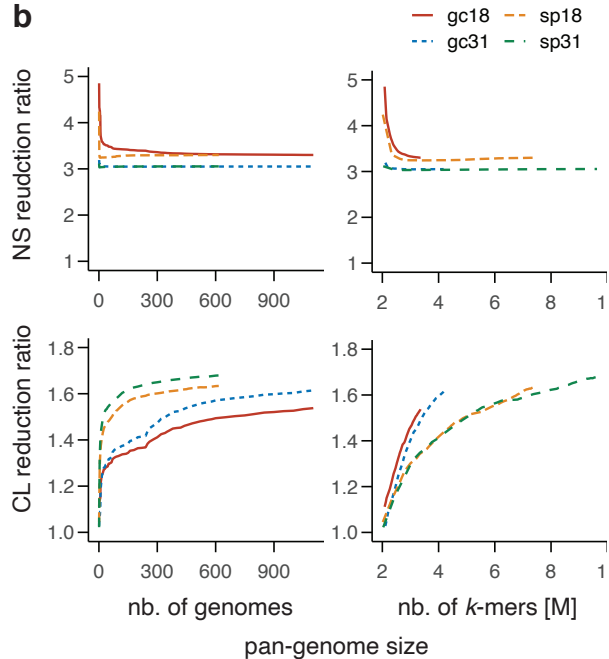760 advances in probabilistic and signal processing algorithms and their application to metagenomics. Nucleic Acids

761 Res [Internet]. 2020; Available from: http://dx.doi.org/10.1093/nar/gkaa265

762 76. Pinho AJ, Ferreira PJSG, Garcia SP, Rodrigues JMOS. On finding minimal absent words. BMC Bioinformatics.
763 2009;10:137.

764 77. Gallant J, Maier D, Astorer J. On finding minimal length superstrings. J Comput System Sci. 1980;20:50–8.

765 78. Manuel P. Revisiting path-type covering and partitioning problems [Internet]. arXiv [math.CO]. 2018. Available
766 from: http://arxiv.org/abs/1807.10613

767 79. Medvedev P, Brudno M. Maximum likelihood genome assembly. J Comput Biol. 2009;16:1101–16.

768 80. Köster J, Rahmann S. Snakemake-a scalable bioinformatics workflow engine. Bioinformatics. 2012;28:2520–2.

769 81. Grad Y. Data for "Genomic Epidemiology of Gonococcal Resistance to Extended-Spectrum Cephalosporins,
770 Macrolides, and Fluoroquinolones in the United States, 2000-2013" [Internet]. Zenodo; 2019. Available from:
771 https://zenodo.org/record/2618836

772 82. Homer N. DWGSIM: Whole Genome Simulator for Next-Generation Sequencing. GitHub repository. 2010;

773 83. Grüning B, Dale R, Sjödin A, Chapman BA, Rowe J, Tomkins-Tinch CH, et al. Bioconda: sustainable and
774 comprehensive software distribution for the life sciences. Nat Methods. 2018;15:475–6.

775

a

Individual k-mers: ACG, CGA, GAA, AAG, AGC, CGT, GTA, TAG, CGG

NS = 9
CL = 27

Maximal unitigs: ACG, CGAAG, CGTAG, AGC, CGG

NS = 5
CL = 19

Maximal simplitigs: ACGAAGC, CGTAG, CGG

NS = 3
CL = 15

b

Compaction

↘ NS
↘ CL

Individual k-mers

Simplitigs

Unitigs

Maximal unitigs

Maximal simplitigs

c

sequence data

k-mers with counts
transformations

k-mers

textual representations

Nucleic acids → Reads → Weighted dBG

Assemblies
Genomes
Transcriptomes
Metagenomes
Pan-genomes

dBG

transformations

Simplitigs

Unitigs

a *S. pneumoniae* **b** *E.coli* **c** *S. cerevisiae*

d *C. elegans* **e** *B. mori* **f** *H. sapiens*

Legend: Unitigs (dashed), Simplitigs (solid), Lower bound (dash-dot)

k-mer length

S. pneumoniae   *E. coli*   *S. cerevisiae*

C. elegans   *B. mori*   *H. sapiens*

- BCALM 2 (1 thread)
- BCALM 2 (4 threads)
- ProphAsm (1 thread)

Mem [GB]

CPU [mins]

k-mer length

a

gc31

Legend: unit (dash-dot) · lobound (long dash-dot) · simpl (solid)

b

Legend: gc18 (red solid) · gc31 (blue dotted) · sp18 (orange dashed) · sp31 (green dashed)

Panel a axes:
- NS [k] vs nb. of genomes
- NS [k] vs nb. of *k*-mers [M]
- CL [Mbp] vs nb. of genomes
- CL [Mbp] vs nb. of *k*-mers [M]

Panel b axes:
- NS reudction ratio vs nb. of genomes
- NS reudction ratio vs nb. of *k*-mers [M]
- CL reduction ratio vs nb. of genomes
- CL reduction ratio vs nb. of *k*-mers [M]

pan-genome size

a

NS [k] (Unitigs, Simplitigs, Assemblies vs *k*-mer length: 19, 23, 27, 31)

CL [Mbp] (Unitigs, Simplitigs, Assemblies vs *k*-mer length: 19, 23, 27, 31)

b

Memory [Mbp] (Unitigs, Simplitigs, Assemblies vs *k*-mer length: 19, 23, 27, 31)

Matching [secs] (Unitigs, Simplitigs, Assemblies vs *k*-mer length: 19, 23, 27, 31)

a

Solid pan-genomes (n=112)

All pan-genomes (n=3,179)

NS [M], CL [Gbp] plotted against *k*-mer length (19, 23, 27, 31) for Unitigs and Simplitigs.

b

Solid – desktop | Solid – cluster | All – desktop | All – cluster

Memory [Gbp], Loading [secs], Matching [secs] plotted against *k*-mer length (19, 23, 27, 31) for Unitigs and Simplitigs.